Journal of Materials Chemistry

Cite this: J. Mater. Chem., 2011, 21, 10448

www.rsc.org/materials

PAPER

A new graphene-modified protic ionic liquid-based composite membrane for solid polymer electrolytes†

Yun-Sheng Ye,[a] Chi-Yung Tseng,[a] Wei-Chung Shen,[a] Jing-Shiuan Wang,[a] Kuan-Jung Chen,[a] Ming-Yao Cheng,[a] John Rick,[a] Yao-Jheng Huang,[b] Feng-Chih Chang[b] and Bing-Joe Hwang*[a]

Received 17th March 2011, Accepted 14th April 2011
DOI: 10.1039/c1jm11152c

The production of a solid polymer electrolyte with high ionic conductivity and mechanical properties is the main fabrication challenge in application of polymer electrolyte membranes. This paper describes a novel polymer electrolyte membrane using protic ionic liquids (PILs) with ionic liquid polymer modified graphene (G) sheets [denoted PIL(NTFSI)-G] that exhibit dramatic enhancements in ionic conductivity (257.4%) and mechanical properties (345% improvement in tensile strength and a near 25-fold increase in modulus were achieved at 150 °C) with a minimal loading of PIL(NTFSI)-G (0.5 wt %). The addition of graphene, by sparing the high-cost PIL addition, gives a 20% cost-saving. The homogeneous distribution of graphene sheets as a 3D network through the polymer matrix in the composite membrane provides a high degree of continuous and interconnected transfer channels to facilitate ion transfer and enhance nanofiller–matrix adhesion to reinforce mechanical properties. This newly developed material provides a potential route toward the design and fabrication of polymer electrolytes.

1. Introduction

Graphene, which comprises a one-atom-thick two-dimensional honeycomb carbon lattice, has attracted increasing attention in recent years, mainly due to its: superior thermal and electrical conductivity, excellent mechanical properties, large specific surface area, and low cost.[1–3] The use of graphene has been explored for various applications such as: electronic and energy storage devices,[4–6] sensors,[7,8] transparent electrodes,[9,10] and nanocomposites.[11,12] Polymer nanocomposites comprising combinations of carbon black, carbon nanotubes (CNTs) and graphene sheets have been seen as potential candidate materials offering the potential to combine several properties, such as: mechanical strength, thermal stability and electrical conductivity. However, graphene sheets provide a more approachable option for forming functional nanocomposites due to the unresolved issues that affect CNTs such as: the tendency of CNTs to agglomerate during processing, the limited availability of high-quality CNTs in large quantities and the high cost of their production.[13,14] The combination of their extraordinary inherent physical properties, combined with their ability to disperse in various polymer matrices, together with their low manufacturing cost (graphite) has led to the creation of cost-effective and high-performance polymer nanocomposites.

Protic ionic liquids (PILs) have attracted considerable attention in recent years due to their interesting and potentially useful physicochemical properties, including their: high ionic conductivities, high polarities, high densities, high heat capacities, and their high thermal and chemical stabilities.[15,16] PILs with these sought after characteristics have been pursued as replacements for liquid electrolytes, which are: toxic, flammable and subject to leaching. One of the main issues needing to be addressed with respect to the development of polymer electrolyte membrane fuel cells (PEMFCs) is the development of membrane materials with high operating temperatures (>100 °C) that show: high reaction kinetics at both electrodes, less poisoning at the anode, and easy heat and water management of the stacks.[17,18] Recently, many studies have been carried out to develop IL-based membranes with high ionic conductivities that can operate at higher temperatures (100–200 °C) in anhydrous conditions.[19–23]

It is well-known that incorporating inorganic fillers into the polymer electrolytes can alter and improve the physical and chemical properties of polymers. In previous studies, membranes modified with nanosized inorganic fillers have exhibited excellent performance and encouraging results.[22,24,25] In addition, the approach of using carbon nanofillers in the polymer electrolyte fuel cells membrane[26,27] has shown a remarkable improvement in membrane performance such as proton conductivity, mechanical properties and methanol permeability, due to the increased sulfonic acid content and better channel-like network for proton transport.[27] Although there have been some recent reports

[a]Department of Chemical Engineering, National Taiwan University of Science and Technology, Taipei, Taiwan. E-mail: bjh@mail.ntust.edu.tw
[b]Institute of Applied Chemisty, National Chiao-Tung University, Hsin-Chu, Taiwan

† Electronic supplementary information (ESI) available. See DOI: 10.1039/c1jm11152c

focused on the properties of IL-based composite membranes, the incorporation of graphene into IL-based membranes has not been reported until now.

The successful preparation of composite polymer electrolytes, however, is critically dependent on the quality of nanofiller dispersion in the polymer matrix, which directly correlates with its effectiveness for improving mechanical, electrical, impermeability, and other properties. The production of a stable dispersion of graphene sheets in ILs is the main fabrication challenge. More recently, the chemical reduction of exfoliated graphene oxide (GO) in the presence of ionic liquid polymer with hydrazine monohydrate, which are well dispersed in ILs has been demonstrated.[28,29] Here we used an ionic liquid polymer to stabilize the isolated graphene sheets and provide functionality for helping the dispersion of graphene sheets between the IL and sulfonated polymer matrix. In addition, the graphene surface is functionalized with ionic liquid groups to obviate possible high intrinsic electronic conduction. More significantly, the mere presence of a minimal amount of the ionic liquid modified graphene (<0.9 wt%) is not adequate to form an electronically conducting network.[30] In this study, we prepared the polymer electrolyte membrane, using protic ionic liquid based composite membranes with ionic liquid modified graphene sheets [PIL(NTFSI)-G], using a simple solution blending method. In these SPI/PIL(NTFSI)-G/PIL composite films, the graphene sheets are uniformly dispersed in the IL-based membrane. Furthermore, the composite film containing graphene (0.5 wt%) exhibited greatly improved ionic conductivity and mechanical properties in comparison with a pure SPI/PIL film.

2. Experimental

Preparation of graphene oxide (GO) and ionic polymer modified graphene

GO was prepared using a modification of Hummers and Offeman's method[31,32] and purified by the centrifugal process—see ESI†. The PIL(Br), poly(1-vinyl-3-butylimidazolium) bromide, was synthesized according to a previously reported procedure.[29] The average molecular weight (M_w) of PIL(Br) is about 150 000 as determined by gel permeation chromatography (GPC). To prepare the ionic polymer modified graphene, 2 mmol of ionic polymer were dissolved in water and added to 20 mL (1.5 mg mL^{-1}) of an aqueous GO suspension. The mixture was then reduced with hydrazine (3.5 mmol) at 90 °C for 1 h under continuous stirring. After reduction, a dispersion of reduced graphene oxide was centrifuged several times to remove residual ionic polymer and then dried at room temperature in vacuum for at 48 h. Reduced graphene oxide (R-G) was synthesized and purified using the same procedure, but without the addition of ionic polymer. Ionic liquid polymer modified graphene sheets [PIL(Br)] were prepared *via* same procedure, and further treated with ionic salts (*i.e.* Li^+NTFSI^- and $Na^+BF_4^-$) to obtain different anion of ionic liquid polymer modified graphene sheets [PIL(NTFSI)-G and PIL(BF_4)-G]. PIL(Br)-G (500 mg) was re-dispersed in 500 mL water to produce an aqueous graphene suspension (1 mg mL^{-1}) and then 3 mmol of lithium bis(trifluoromethylsulfonyl) amide (Li^+NTFSI^-) or sodium tetrafluoroborate ($Na^+BF_4^-$) was added, resulting in dark black precipitates. The dark black precipitates were filtered and dried at room temperature in vacuum for at 48 h.

Preparation of sulfonated polyimide (SPI) and SPI/graphene/IL composite membranes

The sulfonated polyimide (SPI) was synthesized according to our previously reported procedure.[33,34] The properties of the SPI containing 80% hydrophilic units ($n : m = 8 : 2$) are the focus of this study. The IEC of SPI is 2.31 meq g^{-1} (by titration), which is close to the theoretical value 2.49 meq g^{-1}. SPI (0.5 g) were dissolved in 5 mL of DMSO with 10 wt% solid content and stirred at 60 °C for 3 h. A solution comprising different ratios of IL (BMIm-NTFSI), PIL(NTFSI)-G and DMSO (1 mL) was stirred and ultrasonicated to obtain a homogeneous solution, which was then added to SPI/DMSO solution and stirred at 60 °C for 24 h. The SPI/PIL(NTFSI)-G/PIL solution was cast onto a Teflon mold and dried at 75 °C for at least 24 h and then heated at 120 °C to remove any residual solvent.

Characterization

The UV-vis spectra were obtained using a Mecasys optizen 2120 UV spectrometer at room temperature. The ionic conductivity of the membrane was determined with an ac electrochemical impedance analyzer (PGSTAT 30): the experiments involved scanning the ac frequency, from 100 kHz to 10 Hz, at a voltage amplitude of 10 mV. Dynamic mechanical analyses were performed using a DuPont Q800 dynamic mechanical analyzer (DMA) over the temperature range 50–350 °C, using a frequency of 1.0 Hz and a heating rate of 5 °C min^{-1}; data acquisition and analysis of the storage modulus (E') were performed automatically by the system using samples having a length of 14 mm, a width of 5 mm, and a thickness of 0.15 mm. The morphology of the graphene in the composites was observed using a JEOL JEM-1200CX-II transmission electron microscope operated at 120 kV. Scanning electron microscopy (SEM) images were taken with a Hitachi S-4700 microscope using an accelerating voltage of 15 kV. A tensile strength elongation test was carried out using a universal testing machine (EZ-L-500N; SHIMADZU, Kyoto, Japan). The test specimens were carefully cut to have dimensions of 5 mm × 50 mm, and the thickness of each specimen was measured. The testing was measured with a constant crosshead speed of 1 mm min^{-1}.

3. Results and discussion

The ionic polymer graphene sheets (PSS-G, PIL(NTFSI)-G and PIL(BF_4)-G were synthesized in accordance with previously published methods.[28,29,31] We prepared PSS-G sheets *via* the chemical reduction of exfoliated graphene oxide (GO) in the presence of PSS with hydrazine monohydrate.[31] Ionic liquid (IL) polymer modified graphene sheets [PIL(Br)] were prepared using a similar procedure, and further treated with different ionic salts (*i.e.* Li^+NTFSI^- and $Na^+BF_4^-$) to obtain hydrophobic modified graphene sheets [PIL(NTFSI)-G and PIL(BF_4)-G], which can be readily re-dispersed in a wide range of polar aprotic solvents [*e.g.* dimethylformamide (DMF), propylene carbonate (PC), acetonitrile (AN) and dimethyl sulfoxide (DMSO)] upon mild sonication, to form black suspensions.

The formation of GO, R-G and modified graphene suspensions allows the reaction to be monitored by UV-vis spectroscopy, see Fig. S1a†. The GO suspension displayed an absorption maximum at 257 nm, while the reduced GO (R-G) and modified graphene showed a bathochromic shift of the absorption peak to 270 nm upon reduction, along with an increase in the background absorbance. The UV-vis spectrum of the modified graphene possesses similar features to that of the ionic polymer itself (Fig. S1a†), indicating that the ionic polymer is strongly attached to the platelet surface. Fourier transform infrared (FT-IR) spectroscopy in Fig. S1b† gives the characteristic absorption of functional groups and organic molecules on the graphene sheets. While the FT-IR spectrum of GO is quite informative (see ESI†). In comparison to the IR spectrum of GO, those for R-G and modified graphene show a decrease in C=O and C–O stretch intensities, confirming deoxygenation of the graphene sheets after chemical reduction. After modification with ionic polymer, the appearance of new bands corresponding to the SO_3 anion (1189, 1123 cm^{-1}),[31] the NTFSI anion (1125, 1188, 1346 cm^{-1})[28,35] and the BF_4 anion (744 cm^{-1}) for PSS-G, PIL(NTFSI)-G and PIL(BF_4)-G was observed, indicating successful modification and the formation of the corresponding ionic polymer modified graphene.

To monitor the composition of the ionic polymer modified graphene sheets, we employed X-ray photoelectron spectroscopy (XPS) and is shown in Fig. S2a–e†. The C 1s XPS spectrum of GO (Fig. S2a†) clearly indicates a considerable degree of oxidation with four components that correspond to carbon atoms in different functional groups [non-oxygenated ring C (284.6 eV), the C in C–O bonds (286.8 eV), the carbonyl C (C=O, 288.5 eV), and the C (epoxy/alkoxy, 286.1 eV)].[31] The peak intensities of these components (C–O, C=O and C–OH) in the R-G and modified graphene samples are much smaller than those in the GO, indicating considerable de-oxygenation by the reduction process. After modification with ionic polymer, the observation of S 2p at 167.7 eV from PSS-G, the S 2p at 168.7 eV and F 1s at 688.9 eV from PIL(NTFSI)-G, and the F 1s at 686.3 eV and B 1s at 194.2 eV from PIL(BF_4)-G confirms the presence of characteristic polymer anions or cations in the modified graphene sheets.

Thermogravimetry analysis (TGA) was used to determine the ionic polymer content of modified graphene sheets (Fig. S3a†). The difference in char yield value between the modified graphene and R-G indicates that PIL(NTFSI)-G and PIL(BF_4)-G contain ~24% and ~26% polymer, respectively. However, it is difficult to determine the amount of polymer content in PSS-G due to higher char yield value of PSS (Fig. S3b†). Therefore, elemental analysis (EA) was used and indicated that PSS-G contained ~36% polymer as judged by its sulfur content (R-G without any PSS contains no sulfur at all). Fig. S4† provides X-ray diffraction patterns from GO, R-G and modified graphene powder samples. The strong peak at 12.0° in the GO pattern is not present in the R-G pattern, which showed a broad peak at 20.1–30.9°, indicating that aggregation occurred during chemical reduction. Such aggregation is thought to arise from the strong van der Waals interactions between the reduced graphene sheets.[36] The ionic polymer modifications may cause the graphene sheets to stack more loosely, and the interlayer spacing increases. These results indicated that graphene aggregation may be retained during the chemical reduction process in the presence of ionic polymer, yielding single- and multi-layer graphene sheet in the final graphene-modified product.

Fig. 1 shows photographs of the GO, R-G and modified graphene corresponding to DMSO dispersion before and after mixing with BMIm-NTFSI. Obviously, the entire sample was stabilized in the DMSO [Fig. 1, (1)–(5)]. However, with the addition of BMIm-NTFSI, the GO, R-G and PSS-G become unstable and precipitated, *cf.* PIL(NTFSI)-G and PIL(BF_4)-G after deposition for 30 min. This phenomenon may result from the ionic liquid electrolytes neutralizing the charges on the sheets, destabilizing the resulting dispersions.[6] The IL polymer, which has an excellent stabilizing ability with respect to graphene sheets in the presence of IL has also been used to stabilize GO sheets in the presence of IL, see (Fig. S5†), which shows that GO forms a stable dispersion in the presence of IL polymer [PIL(NTFSI)]. Additionally, we measured the UV-vis absorbance of PIL (NTFSI)-G sheets (0.05–0.01 mg mL^{-1}) in BMIm-NTFSI (Fig. 2). The absorbance of the graphene sheets in the IL obeys Beer's law indicating that the dispersion of the graphene sheets in BMIm-NTFSI is homogeneous and no effects could be associated with concentration-dependent aggregation.[29,37] The photographs (Fig. S6†) also show that the color of the ionic liquid polymer modified graphene dispersion in BMIm-NTFSI is not changed noticeably after one month, indicating that the dispersion is very stable. Therefore, we can conclude that the existence of the IL polymer is essential for the dispersion of the graphene sheets in the IL-based membrane system.

Sulfonated polyimide (SPI) is a commonly used polymer, due to its: ease of processing, low cost, and good mechanical properties. An ionic liquid has already been successfully used with SPI for the preparation of a polymer electrolyte.[19,23] Therefore, SPI was chosen as the polymer matrix for the preparation of composite polyelectrolyte membranes in this work. Fig. 3 shows

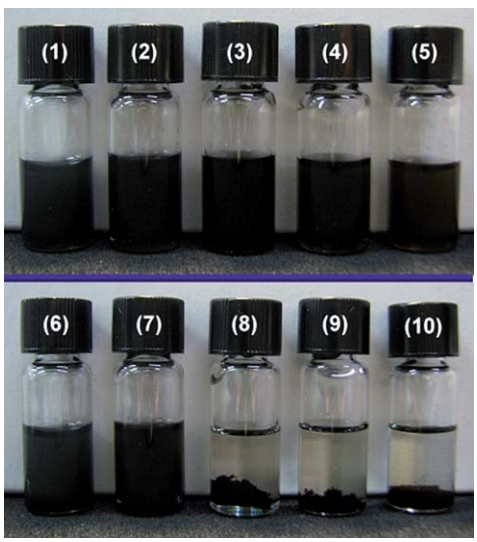

Fig. 1 Photographs of (1)–(5) correspond to DMSO dispersion of the (1) PIL(NTFSI)-G, (2) PIL(BF_4)-G, (3) PSS-G, (4) R-G and (5) GO (0.25 mg mL^{-1}); photographs of (6)–(10) correspond to (1)–(5) after being mixed with BMIm-NTFSI of 2.5 mg by shaking vigorously and then depositing for 30 min.

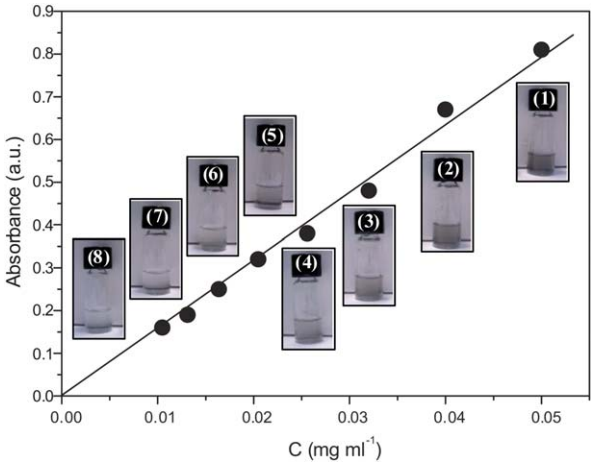

Fig. 2 UV-vis absorption spectra of PIL(NTFSI)-G sheets dispersed in BMIm-NTFSI with different concentrations: 0.05–0.01 mg mL^{-1} dependence of the absorbance on concentration at 600 nm (inset), and the reference solution used in the measurement was neat BMIm-NTFSI.

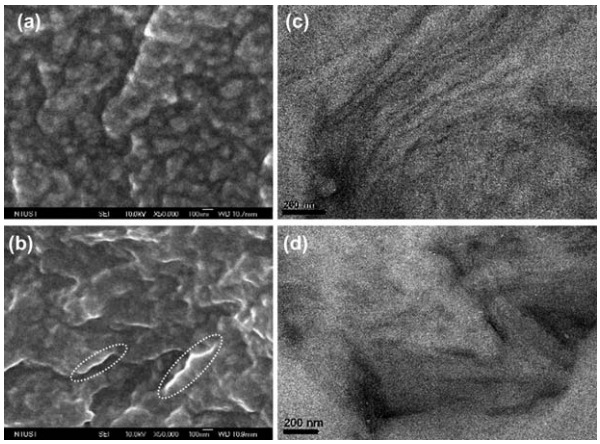

Fig. 4 SEM images of (a) pure SPI/PIL and (b) SPI/PIL(NTFSI)-G/PIL 0.9 wt%; TEM images of SPI/PIL(NTFSI)-G/PIL (c) 0.5 wt% and (d) 0.9 wt%.

photographs of the resulting SPI/PIL(NTFSI)-G/PIL nanocomposite membranes containing various amounts of graphene fillers. These composite membranes are semitransparent (dark yellow), freestanding and flexible; additionally, they can be easily cut into any desired sizes and shapes.

Fig. 4a and b show SEM micrographs of the fractured surfaces of the plain SPI/PIL and SPI/PIL(NTFSI)-G/PIL composite membranes made with 0.9 wt% graphene loading. The bright regions are attributed to high conductivity graphene deposits. It is thought that the graphene nanosheets randomly disperse as a 3D network through the SPI matrix (dark region), and do not just align parallel to the surface of the sample film. Additionally, the TEM images of the SPI/PIL(NTFSI)-G/PIL composite membrane (Fig. 4c) clearly reveal the fully exfoliated graphene nanosheets. Some graphene nanosheets crumple due to their thinness. The homogeneous dispersion of graphene is ascribed to the ionic liquid polymer of PIL(NTFSI)-G, enhancing the interfacial compatibility with BMIm-NTFSI and SPI matrix.

The ionic conductivities (σ) of SPI/PIL(NTFSI)-G/PIL composite membranes, containing 50 wt% BMIm-NTFSI, with various weight ratios of PIL(NTFSI)-G in anhydrous conditions were plotted as a function of temperature (40–160 °C) as shown in Fig. S7†. Interestingly, the incorporation of graphene sheets into the polymer membranes resulted in a considerable increase in the ionic conductivities of the membranes with an increase in the amount of the graphene at all the temperatures examined (40–160 °C); however, it abruptly decreased with the addition of excess graphene. This may be attributed to the homogeneous distribution of graphene sheets as a 3D network through the SPI matrix in the composite membrane creating high degree of continuous and interconnected transfer channels, thereby resulting in higher conductivity. However, with further graphene loading, the blocking effect starts to predominate, thus reducing the conductivity of the composite membrane. Membranes made with same content of PIL(NTFSI)-G (0.5 wt%), with various loadings of PIL (50–80 wt%) at different temperatures (40, 100 and 160 °C), were also prepared and characterized. Fig. S8† clearly shows that with the incorporation of PIL(NTFSI)-G, a lower amount of the PIL (60 wt%) can yield higher conductivity, whereas a higher amount of the PIL (80 wt%) is needed to reach a conductivity value close to that of the plain SPI/PIL membrane at all temperatures. This result indicates the incorporation of graphene enabled the saving of PIL to apply to IL-based membranes to achieve conductivity, together with an approximate 20% saving in PIL. We also examined the role of graphene in improving the ionic conductivity of the SPI membrane by changing the structure of SPI [from SPI(PDDA-BDSA-PMDA) to SPI(PDDA-ODADS-ODPA)] (Scheme S1†). Obviously the incorporation of PIL(NTFSI)-G in the both types of SPI matrix, raises the ionic conductivity of the plain SPI/PIL to about four times that of the SPI/PIL(NTFSI)-G/PIL composite membrane with 0.5 wt% graphene loading at 100 °C (Fig. S9†). Therefore, we can conclude that the exfoliated graphene nanosheet in the IL-based membrane exerts a significant improvement on the ionic conductivity (Fig. 5), while the embedded graphene nanosheets have the ability to facilitate ion transport on their external surfaces and form 3D ion transport channels throughout the membrane (Fig. 6).

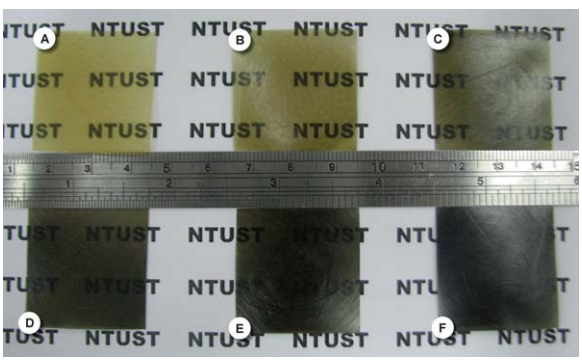

Fig. 3 Photographs of (A) and (B)–(F) correspond to SPI/PIL(NTFSI)-G/PIL composites membranes with PIL(NTFSI)-G loading (B) 0.1, (C) 0.3, (D) 0.5, (E) 0.7 and (F) 0.9 wt%, respectively.

To investigate the effect of the graphene on the mechanical properties of the hybrid membranes, dynamic mechanical

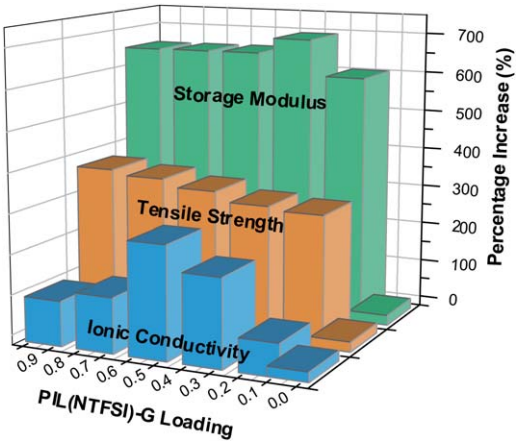

Fig. 5 The percentage increase of membrane incorporated with various weight ratio of PIL(NTFSI)-G.

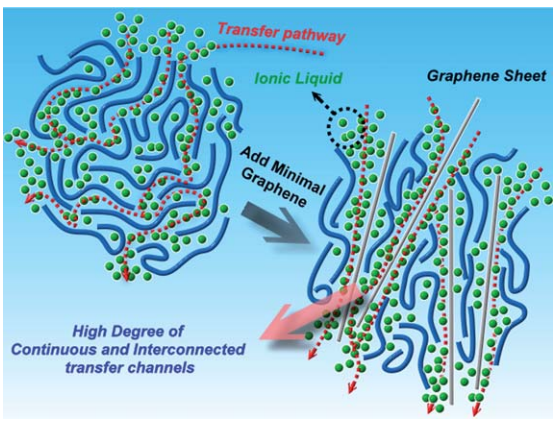

Fig. 6 Illustration on the ion transport mechanism in the membrane.

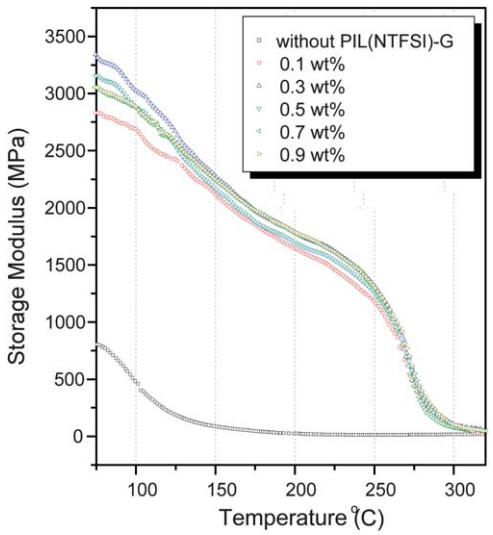

Fig. 7 DMA curves of SPI/PIL(NTFSI)-G/PIL composite membranes.

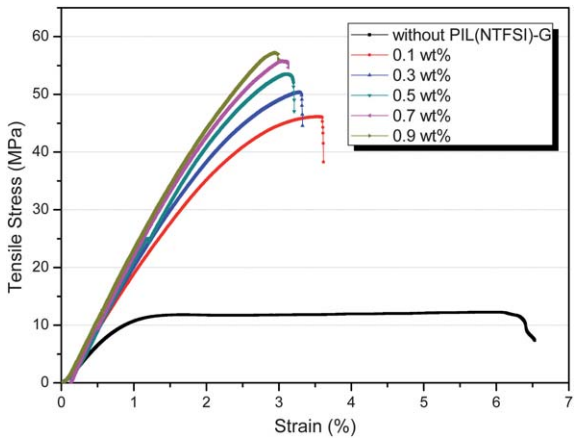

Fig. 8 Stress–strain curve of SPI/PIL(NTFSI)-G/PIL composite membranes.

analysis (DMA) was performed on the composite membrane. Fig. 7 shows the storage modulus of the composite membranes. The storage modulus of the plain SPI/PIL membrane decreased with increasing temperature, reaching the value of 75 MPa at 150 °C. This is comparable to that of IL-based membranes under similar experimental conditions,[20,22,38] indicating the good mechanical properties of the SPI/PIL membrane produced in this study. The addition of graphene sheets into SPI polymer membranes resulted in a remarkable increase in the modulus. It is worth noting that the storage modulus of composite membranes still maintain more than 2200 MPa compared to the plain SPI/PIL membranes at 150 °C. The highest modulus (3040 MPa) was obtained by incorporating 0.3 wt% of PIL(NTFSI)-G in the membrane, this value is about six times that of a plain SPI/PIL membrane (512 MPa) at 100 °C (Fig. 5). And the modulus of SPI/PIL(NTFSI)/IL composite membranes (2100 MPa) is more than 25 times greater than plain SPI/PIL membrane (75 MPa) at 150 °C. This significant improvement in the materials' mechanical properties is a very important factor in the development of membrane materials with high operating temperatures (>100 °C).

Fig. 8 shows the relationship between graphene loading and tensile strength of the composites. It can be seen that the addition of graphene obviously enhances the mechanical properties of the SPI/PIL(NTFSI)-G/PIL composite membrane. The Young's modulus and tensile strength both show continuous improvement with increases in the amount of incorporated graphene, and reach ultimate values of 2.04 GPa and 57.9 MPa respectively, with the incorporation of 0.9 wt% into the composite membrane, corresponding to increases of 127% and 345%, respectively (Fig. 5). The excellent reinforcement of graphene could be attributed to the good dispersion of graphene sheets in composites and the strong interactions between the graphene and the polymer matrix.[11,39] Fig. S10† presents the effect of graphene on the thermal decomposition temperature (T_d) at 10 wt% weight loss. The addition of graphene enhances the thermal stability of the SPI/PIL(NTFSI)-G/PIL composites membrane, which is not significantly affected by the further addition of graphene. The enhancement of the thermal stability attributed to the 2D graphene could act as a gas barrier, which leads to a tortuous pathway for the volatile degradation products, and delays the decomposition of polymer chains at the matrix–filler interface, thereby retarding the whole nanocomposite degradation.[40,41]

Conclusions

A stable dispersion of graphene sheets in BMIm-NTFSI has been successfully prepared by decorating graphene sheets with an ionic liquid polymer. A freestanding, flexible SPI/PIL(NTFSI-G)/IL composite membrane with well-dispersed graphene morphology has been formed by the simple blending of a mixture of SPI, graphene and IL in DMSO. The good dispersion and the strong interface facilitated the high-level reinforcement provided by the extremely small amount of added graphene. The ionic conductivity of a composite membrane, with 0.5 wt% graphene loading, was 7.5×10^{-3} S cm^{-1} at 160 °C, which is approximately four times higher than that of a plain SPI/PIL membrane. The incorporation of graphene, by enhancing conductivity, resulted in a PIL cost-saving of approximately 20%. The modulus (from DMA) of the composite membranes is more than 25 times greater than the plain SPI/PIL membrane at 150 °C. The mechanical properties of the composites membrane show an increase of 127% in Young's modulus, and a 345% increase in tensile strength with the addition graphene (0.9 wt%), in comparison with the plain SPI/PIL membrane. We believe that this approach will open up enormous opportunities that take advantage of the unique properties of graphene for polymer electrolyte applications.

Acknowledgements

Thank for chia-ying chien of Instrumentation Center, National Taiwan University for TEM experiments. We thank financial support from the National Science Council (under contract numbers NSC-99-2120-M-011-001), facilities from the National Taiwan University of Science and Technology, and the National Synchrotron Radiation Research (NSRRC) is gratefully acknowledged.

Notes and references

1 T. Ramanathan, A. A. Abdala, S. Stankovich, D. A. Dikin, M. Herrera Alonso, R. D. Piner, D. H. Adamson, H. C. Schniepp, X. Chen, R. S. Ruoff, S. T. Nguyen, I. A. Aksay, R. K. Prud'Homme and L. C. Brinson, *Nat. Nanotechnol.*, 2008, **3**, 327.
2 D. A. Dikin, S. Stankovich, E. J. Zimney, R. D. Piner, G. H. B. Dommett, G. Evmenenko, S. T. Nguyen and R. S. Ruoff, *Nature*, 2007, **448**, 457.
3 S. Stankovich, D. A. Dikin, G. H. B. Dommett, K. M. Kohlhaas, E. J. Zimney, E. A. Stach, R. D. Piner, S. T. Nguyen and R. S. Ruoff, *Nature*, 2006, **442**, 282.
4 M. D. Stoller, S. Park, Y. Zhu, J. An and R. S. Ruoff, *Nano Lett.*, 2008, **8**, 3498.
5 M. Liang and L. Zhi, *J. Mater. Chem.*, 2009, **19**, 5871.
6 D. Li, M. B. Muller, S. Gilje, R. B. Kaner and G. G. Wallace, *Nat. Nanotechnol.*, 2008, **3**, 101.
7 J. D. Fowler, M. J. Allen, V. C. Tung, Y. Yang, R. B. Kaner and B. H. Weiller, *ACS Nano*, 2009, **3**, 301.
8 F. Schedin, A. K. Geim, S. V. Morozov, E. W. Hill, P. Blake, M. I. Katsnelson and K. S. Novoselov, *Nat. Mater.*, 2007, **6**, 652.
9 X. Li, G. Zhang, X. Bai, X. Sun, X. Wang, E. Wang and H. Dai, *Nat. Nanotechnol.*, 2008, **3**, 538.
10 H. A. Becerril, J. Mao, Z. Liu, R. M. Stoltenberg, Z. Bao and Y. Chen, *ACS Nano*, 2008, **2**, 463.
11 M. A. Rafiee, J. Rafiee, Z. Wang, H. Song, Z.-Z. Yu and N. Koratkar, *ACS Nano*, 2009, **3**, 3884.
12 K. Zhang, L. L. Zhang, X. S. Zhao and J. Wu, *Chem. Mater.*, 2010, **22**, 1392.
13 R. Verdejo, M. M. Bernal, L. J. Romasanta and M. A. Lopez-Manchado, *J. Mater. Chem.*, 2011, **21**, 3301.
14 H. Kim, A. A. Abdala and C. W. Macosko, *Macromolecules*, 2010, **43**, 6515.
15 N. V. Plechkova and K. R. Seddon, *Chem. Soc. Rev.*, 2008, **37**, 123.
16 O. Green, S. Grubjesic, S. Lee and M. A. Firestone, *Polym. Rev.*, 2009, **49**, 339.
17 M. S. Dresselhaus and I. L. Thomas, *Nature*, 2001, **414**, 332.
18 K. D. Kreuer, S. J. Paddison, E. Spohr and M. Schuster, *Chem. Rev.*, 2004, **104**, 4637.
19 S.-Y. Lee, T. Yasuda and M. Watanabe, *J. Power Sources*, 2010, **195**, 5909.
20 M. A. B. H. Susan, T. Kaneko, A. Noda and M. Watanabe, *J. Am. Chem. Soc.*, 2005, **127**, 4976.
21 Y.-S. Ye, M.-Y. Cheng, J.-Y. Tseng, G.-W. Liang, J. Rick, Y.-J. Huang, F.-C. Chang and B.-J. Hwang, *J. Mater. Chem.*, 2011, **21**, 2723.
22 B. Lin, S. Cheng, L. Qiu, F. Yan, S. Shang and J. Lu, *Chem. Mater.*, 2010, **22**, 1807.
23 S.-Y. Lee, A. Ogawa, M. Kanno, H. Nakamoto, T. Yasuda and M. Watanabe, *J. Am. Chem. Soc.*, 2010, **132**, 9764.
24 F. Pereira, K. Vallé, P. Belleville, A. Morin, S. Lambert and C. Sanchez, *Chem. Mater.*, 2008, **20**, 1710.
25 T. Yamaguchi, H. Zhou, S. Nakazawa and N. Hara, *Adv. Mater.*, 2007, **19**, 592.
26 Z. Chai, C. Wang, H. Zhang, C. M. Doherty, B. P. Ladewig, A. J. Hill and H. Wang, *Adv. Funct. Mater.*, 2010, **20**, 4394.
27 R. Kannan, B. A. Kakade and V. K. Pillai, *Angew. Chem.*, 2008, **120**, 2693.
28 T. Kim, H. Lee, J. Kim and K. S. Suh, *ACS Nano*, 2010, **4**, 1612.
29 X. Zhou, T. Wu, K. Ding, B. Hu, M. Hou and B. Han, *Chem. Commun.*, 2010, **46**, 386.
30 H. J. Salavagione, G. Martinez and M. A. Gomez, *J. Mater. Chem.*, 2009, **19**, 5027.
31 S. Stankovich, R. D. Piner, X. Chen, N. Wu, S. T. Nguyen and R. S. Ruoff, *J. Mater. Chem.*, 2006, **16**, 155.
32 W. S. Hummers and R. E. Offeman, *J. Am. Chem. Soc.*, 1958, **80**, 1339.
33 C.-Y. Tseng, Y.-S. Ye, J. Joseph, K.-Y. Kao, J. Rick, S.-L. Huang and B.-J. Hwang, *J. Power Sources*, 2011, **196**, 3470.
34 Y.-S. Ye, Y.-J. Huang, C.-C. Cheng and F.-C. Chang, *Chem. Commun.*, 2010, **46**, 7554.
35 M. K. Mistry, S. Subianto, N. R. Choudhury and N. K. Dutta, *Langmuir*, 2009, **25**, 9240.
36 M. Fang, K. Wang, H. Lu, Y. Yang and S. Nutt, *J. Mater. Chem.*, 2009, **19**, 7098.
37 V. A. Sinani, M. K. Gheith, A. A. Yaroslavov, A. A. Rakhnyanskaya, K. Sun, A. A. Mamedov, J. P. Wicksted and N. A. Kotov, *J. Am. Chem. Soc.*, 2005, **127**, 3463.
38 S. Subianto, M. K. Mistry, N. R. Choudhury, N. K. Dutta and R. Knott, *ACS Appl. Mater. Interfaces*, 2009, **1**, 1173.
39 X. Zhao, Q. Zhang, D. Chen and P. Lu, *Macromolecules*, 2010, **43**, 2357.
40 Y. Wang, Z. Shi, J. Fang, H. Xu, X. Ma and J. Yin, *J. Mater. Chem.*, 2011, **21**, 505.
41 N. G. Sahoo, S. Rana, J. W. Cho, L. Li and S. H. Chan, *Prog. Polym. Sci.*, 2010, **35**, 837.